SAND2015-2512C

Understanding the Run-out Behavior of a Ag-Cu-Zr Braze Alloy When Used to Join Alumina to an Fe-Ni-Co Alloy

P.T. Vianco,* C.A. Walker, D. De Smet, A. Kilgo, B.M. McKenzie, P.M. Kotula, and R.L. Grant
Sandia National Laboratories
Albuquerque, NM USA
**505-844-3429; ptvianc@sandia.gov*

Abstract

The run-out phenomenon occurs when a significant portion of the molten filler metal exits the gap region and accumulates on an exterior, base material surface. Run-out can cause excessive void formation due to the loss of filler metal from gap volume. It can also create stress concentrations that lead to base material cracking, especially when the latter is a brittle material – e.g., ceramics and glasses. At first, run-out appears to result from simply the physical displacement of too-much filler metal for the final gap dimensions (thickness and footprint). On the other hand, an active braze application was investigated that showed run-out to result from an instability in the wetting and spreading process. The filler metal, 97Ag-1Cu-2Zr (wt.%), was used to join an alumina (Al_2O_3) ceramic to a Kovar™ base material. The driving force for run-out was the metallurgical reaction between the Fe, Ni, and Co constituents of Kovar™ with the elemental Al released by the reduction-oxidation reaction between Zr and Al_2O_3. A constraining factor is the surface tension of the molten filler metal in conjunction with the brazement geometry. Based on this study, a modification to the filler metal composition, or use of a barrier coating on the Kovar™ surface, would provide the most promising mitigation strategies against run-out.

Introduction

Run-out Phenomenon

The optimization of a braze joint requires that close control be maintained of the amount of filler metal supplied to the gap. Too little filler metal results in voids and non-filled regions of the brazement that can jeopardize both strength and hermeticity properties. On the other hand, having an excess quantity of filler metal causes the molten braze alloy to be ejected from the gap and collect on an exterior surface as *run-out*. The run-out filler metal may wet to ancillary structures beyond the joint or freeze to non-wettable surfaces. An example of the adhesion of filler metal run-out to base material surfaces is shown in Fig. 1a where the 97Ag-1Cu-2Zr (wt.%, abbreviated Ag-Cu-Zr) filler metal ran out from the joint made between Kovar™ (trademark of Carpenter Technologies, Reading, PA) and an alumina (Al_2O_3) ceramic. The scanning electron microscope (SEM) image in Fig. 1b shows a cross section view of the excess filler metal.

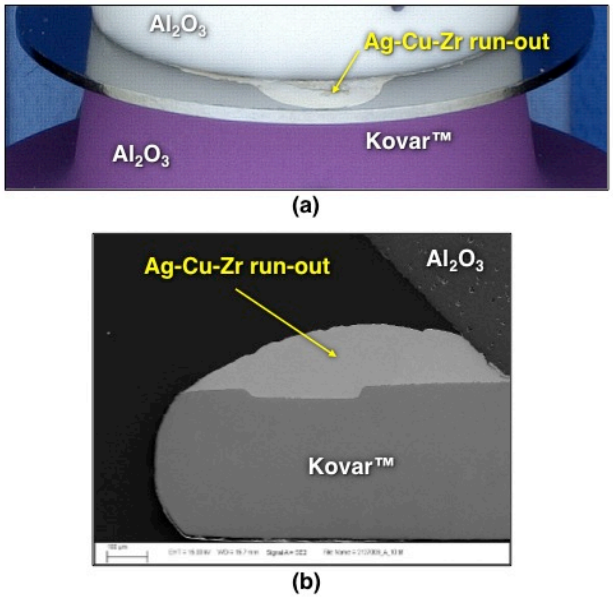

Figure 1 (a) Photograph shows run-out by a Ag-Cu-Zr active braze alloy being used to join two Al_2O_3base materials to a Kovar™ spacer. (b) An SEM photograph was taken of run-out made visible by the metallographic cross section.

There can be significant consequences to a run-out event in terms of braze joint performance. Run-out "blobs" or "lobes" can pose unsightly cosmetic defects or serve as an impediment to visual and x-ray inspection. When the excess filler metal collects outside of the gap, upon solidification, it can interfere with next-assembly fit-up and mechanical functions. Run-out removes filler metal from the joint that can lead to reduced mechanical strength and a potential loss of hermeticity. Poor strength and non-hermeticity may be further aggravated by excessive solidification shrinkage, which contributes to an undersupply of filler metal within the confined geometry of the gap. The latter circumstance is illustrated in Fig. 2a. The inset image shows, what appears to be, excessive void development in the braze joint. However, upon closer analysis, the voids were actually caused by solidification shrinkage enhanced through the loss of filler metal due to run-out.

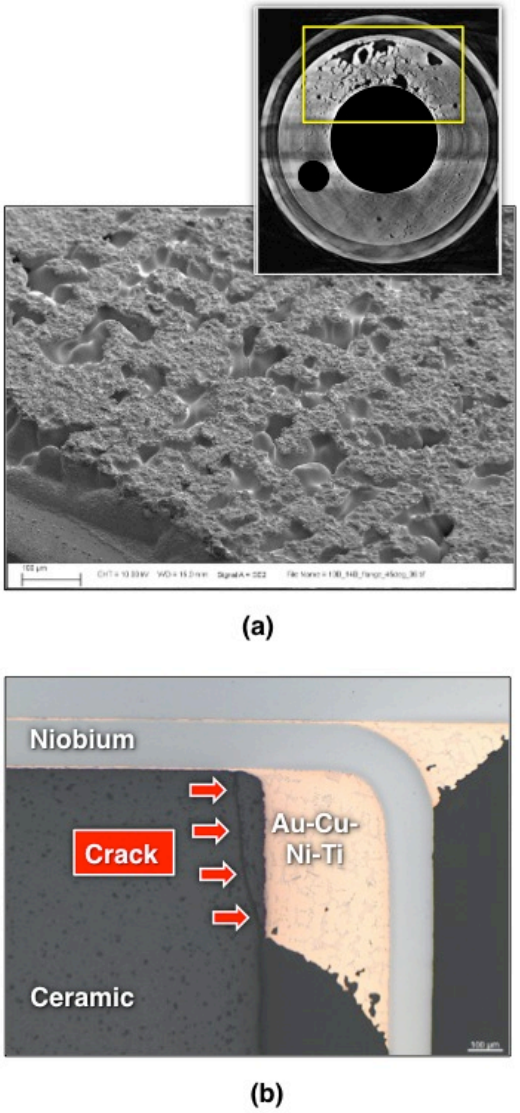

Figure 2 (a) SEM photographs illustrate the voids created by the combination of Ag-Cu-Zr filler metal lost to run-out and solidification shrinkage of the remaining braze alloy. (b) Optical micrograph shows a crack in the ceramic base material due to the run-out of the Au-Cu-Ni-Ti filler metal.

Perhaps the most problematic consequence of run-out is the generation of residual stresses in the base material. This phenomenon is illustrated by the optical micrograph in Fig. 2b. The run-out of a Au-Cu-Ni-Ti filler metal caused cracking in the ceramic member of the assembly. The high stress condition created by the run-out was confirmed by computational modeling, the results of which, are shown in Fig. 3. The run-out and no-run-out braze joints are shown by the optical micrographs in Figs. 3a and 3b, respectively. Finite element models were built from those images; they are shown in Figs. 3c and 3d, respectively. The stress contours predicted by the constitutive model are show in Figs. 3e and 3f for the run-out and no-run-out conditions, respectively. When run-out is present, a peak stress of 42,000 psi is generated in the ceramic, which is more than enough to cause a crack. That stress decreases to the relatively benign 4,400 psi when run-out was absent.

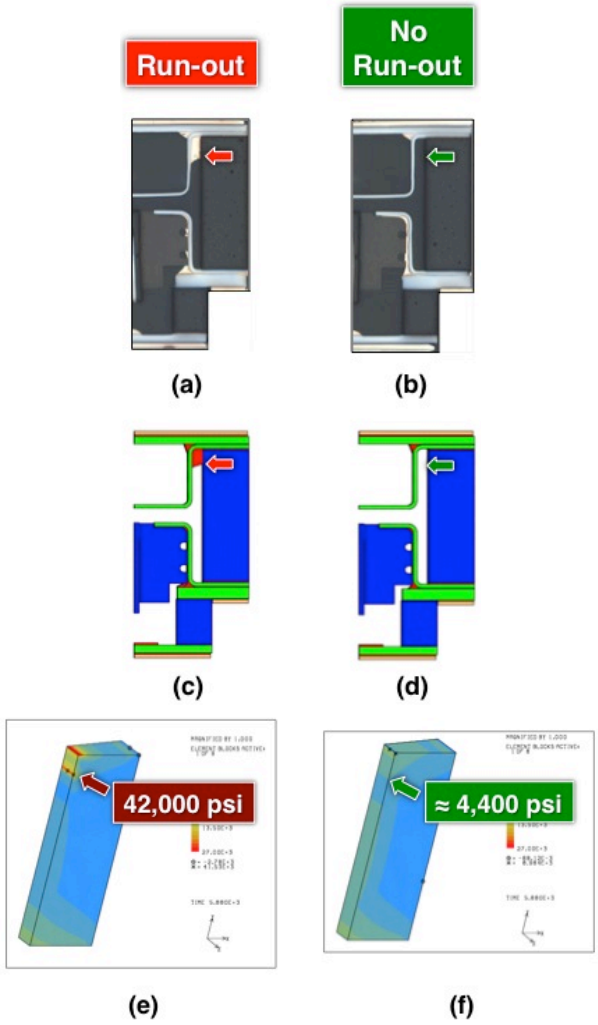

Figure 3 (a, b) Optical micrographs of Au-Cu-Ti-Ni braze joints between Nb and ceramic for which run-out was present or absent. (c, d) Finite element models of the run-out and no-run-out cases used to predict the residual stresses. (e, f) Tensile stress contours and maximum values predicted by the constitutive model for the two conditions.

The aforementioned consequences of run-out have long been recognized by the brazing industry. Several mitigation approaches have been explored to control excessive filler metal flow. One approach is to reduce the peak brazing temperature in order to increase the viscosity of the molten filler metal. The only filler metals for which this approach has merit, are those alloys that have an extended pasty range. When the filler metal has a significant difference between the solidus and liquidus temperatures, $T_l - T_s > 10C$, there is sufficient margin in a typical furnace process to control the filler metal flow properties by strategically selecting a peak temperature that is within the alloy pasty zone. Unfortunately, molten metal viscosity, alone, is not very sensitive to temperatures above the liquidus point. Thus, in the case of eutectic or near-eutectic filler metals ($T_l - T_s < 10C$), altering the brazing temperature offers little control over the flow behavior of the liquid filler metal.

A second approach is to add one or more alloying elements to the filler metal. The goal is to create a wider pasty range in order to allow the process temperature to provide a measure of control on filler metal flow. However, altering the filler metal composition comes with it, many other, often synergistic effects that can degrade braze joint manufacturability, performance, and reliability.

A third strategy is to modify the *geometry* of the base material surface. Adding corners to the base material surface would be expected to slow or halt the flow of molten filler metal. In fact, such a feature is observed in Fig. 1b. The trough was added to the Kovar™ base material to "capture" the filler metal and minimize further run-out. Clearly, the trough technique was not successful.

All of these measures have met with little or no success to control filler metal flow. Their lack of effectiveness, however, suggested that other driving forces were responsible for the run-out behavior, not simply a physical displacement of molten filler metal.

As a summary, there are significant consequences to the run-out phenomenon that extend beyond simply "wasted" filler metal. Run-out can interfere with next-assembly function as well as lead to the damage of adjoining base materials. The inability of early mitigations steps to control run-out provides an indication that this behavior is not simply the physical displacement ("squishing out") of excess molten filler metal from the brazement.

Characterization of Run-out for the Target Application

The Ag-Cu-Zr active braze alloy was considered for an application that required that a Kovar™ structure be joined to an Al_2O_3 ceramic part. The tensile button configuration was used to initially assess braze joint strength, hermeticity, and microstructure prior to the development of actual hardware [1]. A photograph of the tensile button specimen is shown in Fig. 4. Two Al_2O_3 "buttons" were brazed to a Kovar™ "spacer." The spacer had 0.0015 in. dimples that controlled the thicknesses of both gaps. The Ag-Cu-Zr filler metal was in the form of an annular ring. Its footprint was the same as that of the Al_2O_3 faying surface: 0.400 in. inner diameter (ID) and 0.625 in. outer diameter (OD). The preform was 0.002 in. thick. There were two varieties of Al_2O_3 ceramics that are distinguished by their different colors. The small compositional differences responsible for the color variations did not have an effect on any properties investigated in this study.

Shown in each of Figs. 5a and 5b is one-half of two, post-tested, tensile buttons. Both samples were brazed at 965°C for 20 min in a 600 torr Ar atmosphere. The yellow dashed circles indicate the boundaries of the faying surface area. The specimens exhibited significant filler metal run-out as indicated by the arrows. Although two run-out "lobes" formed in Fig. 5a, most often, there was only one per side of the Kovar™ spacer. The run-out lobe on one side did not exhibit a particular correlation with the lobe on the other side.

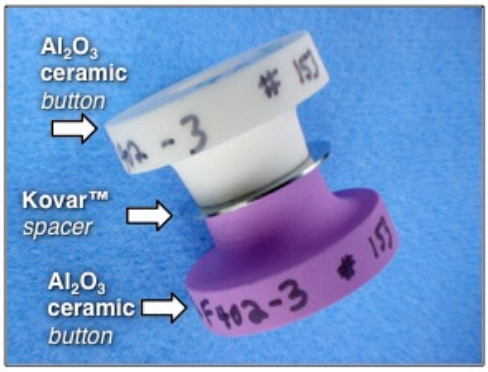

Figure 4 Photograph shows the tensile button configuration. There are two Al_2O_3 ceramic buttons brazed to each of the two sides of the Kovar™ spacer.

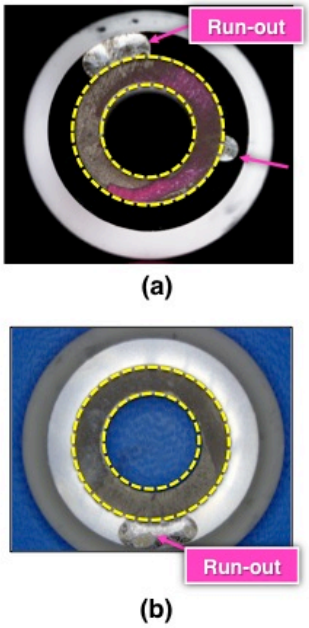

Figure 5 (a, b) Optical photographs show run-out (arrows) experienced by the Kovar™ spacer/Ag-Cu-Zr/Al_2O_3 braze joint. The tensile buttons was brazed at 965°C for 20 min in 600 torr Ar prior to being pull tested; the faying surface is between the dashed circles.

An experiment was performed to explore the possibility that run-out was not simply the ejection of excess filler metal from the joint. A smaller footprint of filler metal was placed in the same tensile button braze joint, by reducing the OD of the Ag-Cu-Zr preform from 0.625 in. to 0.500 in. One tensile button was assembled with a single such preform in the joint. The smaller OD reduced the filler metal volume by 60% so that any occurrence of run-out could not be attributed to a physical displacement effect.

A second tensile button sample was made with *two* of these preforms. The preforms were stacked upon one-another, which in effect, returned to overall solder volume to approximately equal to that of the single preform of nominal OD (0.625 in.). The purpose of the latter specimen was to

determine if run-out was encouraged by a strong degree of capillary flow by the molten filler metal.

Both tensile buttons were brazed at 985°C for 5 min (600 torr Ar). The temperature and time were higher and shorter, respectively, than the nominal conditions. Nevertheless, they were still well within the process window for this filler metal. The tensile buttons were subsequently pull tested to facilitate the documenting of the run-out behavior.

Figure 6 shows optical micrographs that were taken of post-pull tested samples. The run-out is identified by the arrows. The tensile button in Fig. 6a, which had one preform, showed three primary run-out lobes and several lesser wetting fronts. The fact is that run-out took place under this circumstance of limited filler metal decouples the phenomenon from a physical displacement of molten filler metal.

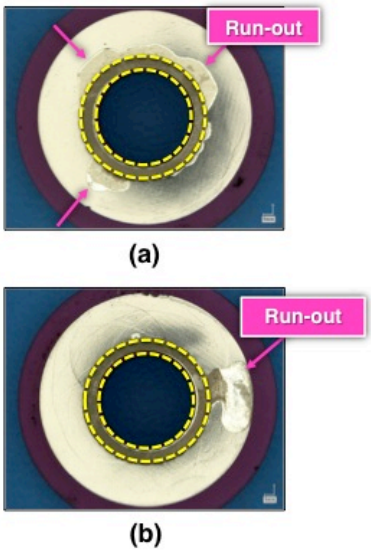

Figure 6 Optical photographs show run-out (arrows) experienced by the Kovar™ spacer/Ag-Cu-Zr/Al_2O_3 braze joint. The process conditions were 985°C for 5 min in a 600 torr Ar atmosphere. (a) This sample was fabricated with a single Ag-Cu-Zr preform having a reduced OD of 0.500 in. (b) This specimen was fabricated with the same, smaller preform footprint, but having two preforms stacked upon each other. The run-out is identified by the arrows.

The tensile button shown in Fig. 6b, which had two preforms, exhibited only a single run-out lobe. That run-out lobe was relatively voluminous, indicating that it carried the excess filler metal of the two preforms. Nevertheless, it occurred in a *single* location indicative of run-out, as opposed to there being a general flow of excess filler metal squished out over a larger area of the Kovar™ spacer surface.

In summary, the experimental evidence showed that the molten filler metal did not respond to changes of volume in a manner that would indicated that run-out was a physical displacement of excessive filler metal. Rather, run-out appeared to result from an instability in the wetting and spreading behavior of molten Ag-Cu-Zr on the Kovar™ base material. The goal of the study described in this report was to collect evidence that could lead to a root-cause determination for run-out. The effort remained with the Ag-Cu-Zr active filler metal and base materials, Kovar™ and Al_2O_3. A longer term objective is to use the root-cause knowledge to develop a first-principles methodology to mitigate against the run-out phenomenon.

Material Systems

The materials systems is the same as that used to exemplify the run-out phenomenon in the previous section. The filler metal is the active braze alloy, 97Ag-1Cu-2Zr (wt.%, abbreviated Ag-Cu-Zr). The filler metal preforms had these dimensions: 0.400 in. ID; 0.625 in. OD, and 0.002 in. thickness. The base materials were (a) the Kovar™ alloy (b) the 94% Al_2O_3 ceramic. The nominal braze process had a peak temperature of 985°C; time duration of 5 min at peak temperature; and a 600 torr Ar atmosphere. The braze joint microstructure is exemplified by the SEM image in Fig. 7. Besides the filler metal and base materials, the brazements were characterized by distinct reaction structures at the two interfaces. Because those structures are critical to the analysis, they are described in greater detail in the next section.

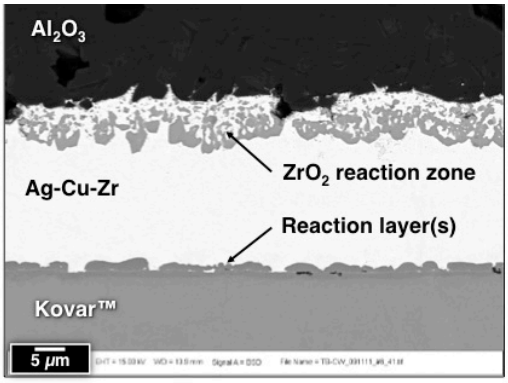

Figure 7 SEM photograph shows the general microstructure of the braze joint that formed between the Kovar™ and Al_2O_3 ceramic base materials using the Ag-Cu-Zr active filler metal. The process conditions were 985°C; 5 min; and 600 torr Ar atmosphere.

Interface Reactions

Cross Section Microstructure

A detailed discussion is presented here of the reaction layers that develop at the Ag-Cu-Zr/Al_2O_3 and Ag-Cu-Zr/Kovar™ interfaces. These reactions form the basis for understanding the run-out phenomenon. The reaction zone created at the Ag-Cu-Zr/Al_2O_3 interface is shown in Fig. 8a. The reaction zone is a coalescence of ZrO_2 particles that developed, initially, at the immediate Ag-Cu-Zr/Al_2O_3 interface as shown in Fig. 8b. The particles separated from the interface and migrated into the near-interface filler metal. The ZrO_2 particles are a product of the reduction-oxidation (redox) reaction between Zr and Al_2O_3 ceramic below:

$$3Zr + 2Al_2O_3 = 4Al + 3ZrO_2 \qquad (1)$$

The reaction is *not* spontaneous, having a calculated Gibb's free energy of +610 cal. This magnitude of free energy is well within the error of literature data so that the reaction may very well be spontaneous (negative), albeit, perhaps only slightly so. Regardless, the redox reaction does, in fact, take place as is evidenced by the appearance of the ZrO_2 zone. The Cu component of the filler metal does not have a role in this reaction; rather, it remained homogeneously-distributed throughout the bulk Ag-Cu-Zr alloy.

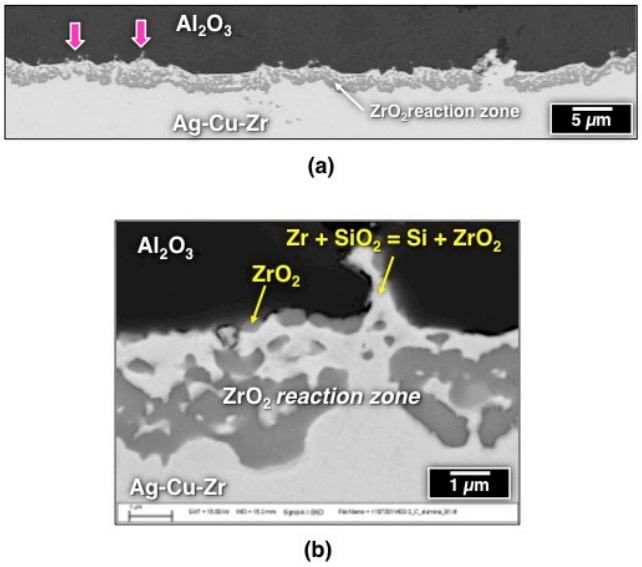

Figure 8 (a) Low magnification SEM photograph shows the ZrO_2 reaction zone at the Ag-Cu-Zr/Al_2O_3 interface. The magenta arrows indicate locations where the Zr/SiO_2 redox reaction removed SiO_2 grain boundary glassy phase, thereby allowing filler metal to infiltrate between the Al_2O_3 grains. (b) High magnification view of the immediate Ag-Cu-Zr/Al_2O_3 interface showing formation of the ZrO_2 particles and infiltration of the inter-grain region by the filler metal as SiO_2 is lost to the Zr/SiO_2 redox reaction.

The ceramic has grain boundary phase based on the SiO_2 glass that bonds the Al_2O_3 grains, together. There is a corresponding redox reaction between the SiO_2 phase and Zr:

$$Zr + SiO_2 = Si + ZrO_2 \qquad (2)$$

This reaction is predicted to be spontaneous because it has a negative Gibb's free energy, -46,100 cal. The evidence of this redox process is replacement of glass material from between the Al_2O_3 grains with filler metal. This effect occurred in Fig. 8a at sites indicated by the magenta arrows and is shown at high magnification in Fig. 8b.

Aside from the fidelity of the reference information, there are three physical phenomena that could drive the Zr/Al_2O_3 redox reaction into spontaneity:

a. Zr/SiO_2 redox reaction,
b. Free energy of solution as elemental Al enters the molten Ag-Cu-Zr filler metal, and
c. Reactions at the Kovar™/Ag-Cu-Zr interface.

It is unlikely that (a) would pose a significant effect given the limited quantity of SiO_2 present in the ceramic. Scenario (b) could potentially contribute to the driving force. The Ag-Al binary alloy phase diagram exhibits a eutectic composition of 71Ag-29Al (wt.%) that has a eutectic temperature of 567°C, which is well below the brazing temperature [2]. That property, together with the extensive composition range in the δ phase (Ag terminal phase) favors a low energy barrier for the dissolution of Al into the molten filler metal. If this scenario did not contribute to the driving force for the Zr/Al_2O_3 redox reaction, it would be *unlikely* to impede it.

The scenario (c) could provide a significant contribution of driving force in support of the Zr/Al_2O_3 redox reaction. Although there is not a particularly strong driving force for Ag to react with the Fe, Ni, or Co constituents of Kovar™, there is an affinity between those elements and Al because they readily form covalent (intermetallic) compounds [3].

The reaction that takes place at the Kovar™/Ag-Cu-Zr interface is illustrated in Fig. 9. The SEM image in Fig. 9a shows the interface microstructure. The sub-layers were identified using energy dispersive x-ray (EDX) as well as elemental spectral analysis. The latter method, the results of which shown in Fig. 9b, uses a thin section formed by focused ion beam (FIB) milling and then analyzed by transmission electron microscopy (TEM) techniques. (Note the magnification marker.) Neither technique included the standards and calibrations necessary to quantify the compositions. Clearly, the Al released by the redox reaction at the Ag-Cu-Zr/Al_2O_3 interface was integral to the Kovar™/Ag-Cu-Zr interface microstructure.

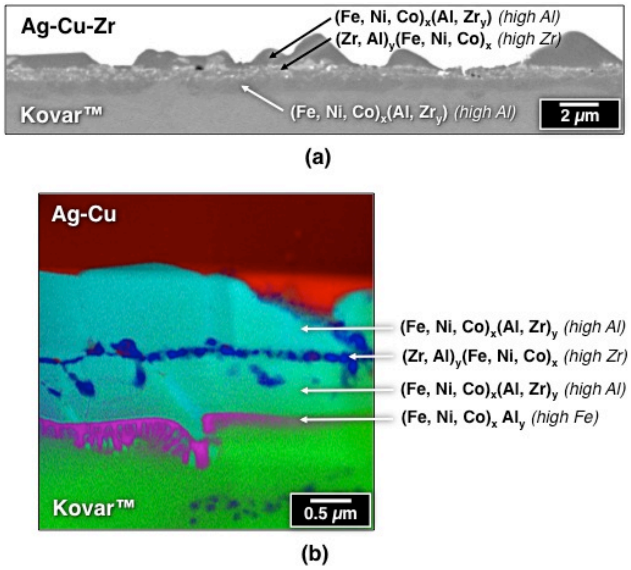

Figure 9 (a) SEM image shows the reaction sub-layers that form at the Kovar™/Ag-Cu-Zr interface in the braze joint fabricated under nominal brazing conditions (985°C, 5min, 600 torr Ar). (b) Elemental spectral analysis shows a map of elements that comprise the reaction sub-layers at the Kovar™/Ag-Cu-Zr interface.

A qualitative accounting was made of the sub-layers as follows: There is the high-Al, $(Fe, Ni, Co)_x(Al, Zr)_y$ layer that

borders with the bulk filler metal (Ag-Cu). Below it is the Zr-rich, $(Zr, Al)_y(Fe, Ni, Co)_x$ layer and underneath it, a second, Al-rich reaction sub-layer also denoted as $(Fe, Ni, Co)_x(Al, Zr)_y$. The fourth and final layer, which is next to the Kovar™ base material, is high in Fe and has a dendritic morphology. That layer was designated as $(Fe, Ni, Co)_xAl_y$. Lastly, it was observed that Cu was not detected in any of the reaction sub-layers; it remained dispersed in the filler metal.

The presence and morphologies of the sub-layers varied somewhat, sample-to-sample, as well as location-to-location along the same interface. The two high-Al reaction sub-layers were general present, but to varying thicknesses. The Fe-rich, $(Fe, Ni, Co)_xAl_y$ layer was observed more infrequently. The high-Zr layer was also typically observed, but having different morphologies, depending on the local availability of Zr. The somewhat diffuse structure, which is exemplified in Fig. 9a, was the norm. In the event that more Zr was available from the filler metal – e.g., in a fillet – then, a thick, continuous reaction layer would replace the diffuse structure at the interface.

Based upon observations compiled from countless cross section analyses, a scenario was formulated that describes the development of the reaction layers at the two interfaces. Experimental data indicate that this process is relatively insensitive to brazing parameters within the nominal process window of [965°C, 995°C] and (5 min, 20 min] for this filler metal. If fact, these reactions occur so rapidly that they cannot be controlled within these parameter ranges. Certainly, a contributing factor to the quickness of the reactions was the fact that all diffusion takes place across the *molten* filler metal.

That sequence is described, using Fig. 10. Captions are provided underneath the pictures. The analysis will assume that the sub-layers that form at the Ag-Cu-Zr/Kovar™ interface, do so sequentially. It is plausible that a sub-layer

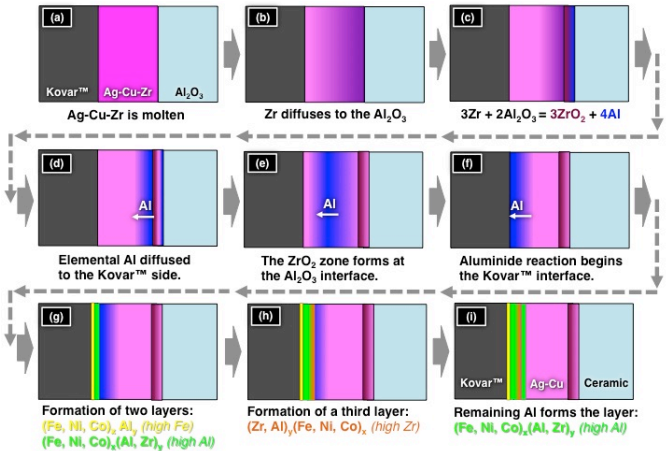

Figure 10 Diagram that depicts the proposed sequence whereby the reaction layers are formed at the Ag-Cu-Zr/Kovar™ and Ag-Cu-Zr/Al_2O_3 interfaces.

could develop from a reaction between two pre-existing sub-layers. A validation of this scenario was beyond the scope of this particular study.

The proposed scenario is described, below:

(a) The molten Ag-Cu-Zr alloy contacts the Kovar™ and Al_2O_3 base materials.

(b) Immediately, Zr diffuses to the latter.

(c) At the Ag-Cu-Zr/Al_2O_3 interface, the redox reaction releases elemental Al into the filler metal.

(d-f) The elemental Al diffuses to the Ag-Cu-Zr/Kovar™ interface and reacts with the Fe-, Ni-, and Co-components of Kovar™ to begin formation of the reaction layers described earlier in Fig. 9.

(g) The high Fe, $(Fe, Ni, Co)_xAl_y$ layer forms adjacent to the Kovar™ base material. Between that layer and the molten Ag-Cu-Zr alloy grows the high Al, $(Fe, Ni, Co)_x(Al, Zr)_y$ reaction layer.

At this point, Zr participates in the Ag-Cu-Zr/Kovar™ interface reactions. This observation implies one of two scenarios: (1) There is an excess of Zr in the molten filler metal because the redox reaction did not consume it all at the Ag-Cu-Zr/Al_2O_3 interface or (2) the presence of the $(Fe, Ni, Co)_xAl_y$ drives the $(Fe, Ni, Co)_x(Al, Zr)_y$ reaction that competes with the redox reaction for Zr in the filler metal.

(h) The driving force for Zr to react at the Ag-Cu-Zr/Kovar™ interface increases as is evidenced by formation of the Zr-rich, $(Zr, Al)_y(Fe, Ni, Co)_x$ reaction layer.

(i) The Zr reaction slows and the remaining Al in the filler metal is used to complete the Ag-Cu-Zr/Kovar™ interface reaction. The same high Al, $(Fe, Ni, Co)_x(Al, Zr)_y$ reaction layer forms at the filler metal interface. The EMPA technique confirmed that Al was absent from the filler metal to within the detection limits of that method (±0.5 wt.%).

The Cu constituent of the Ag-Cu-Zr alloys does not have a detectable presence in *any* of the interface reaction stochiometries. The EPMA determined that the remaining filler metal had retained all of the nominal 2 wt.% Cu concentration as well as confirmed the absence of Zr and Al to within the detection limit.

In summary, the Kovar™/Ag-Cu-Zr/Al_2O_3 materials system was investigated for the reactions that take place at the mutual interfaces. The Zr/Al_2O_3 redox reaction occurred at the Ag-Cu-Zr/Al_2O_3 interface as evidenced by the formation of ZrO_2 reaction zone and the release of elemental Al. The proposed reaction sequence was also predicted at the Ag-Cu-Zr/Kovar™ interface. The layers are a product of reactions between Zr, Al, Fe, Ni, and Co. The completeness of these reactions was confirmed by the absence of both elemental Al and Zr from the filler metal.

Wetting Front Metallurgy

The above discussion demonstrated that aluminide and zirconide reactions, which have very strong driving forces, take place at the Ag-Cu-Zr/Kovar™ interface. The role that those reactions have in the wetting and spreading behavior of this system, was examined in order to find a correlation, if any, between them and the run-out phenomenon. The analysis began by examining the wetting edge of the Ag-Cu-Zr alloy on the Kovar™ base material.

Shown in Fig. 11a is a tensile button that was pull tested to reveal the run-out of the Ag-Cu-Zr filler metal. The yellow box indicates the location of run-out and the microanalysis. Figure 11b is a secondary electron (SE), SEM image of the edge of the run-out. The bulk filler metal formed a lip by lifting from the surface. Because the surface under the lip does not appeared fractured, the lip was formed by a retraction of the bulk Ag-Cu-Zr during solidification.

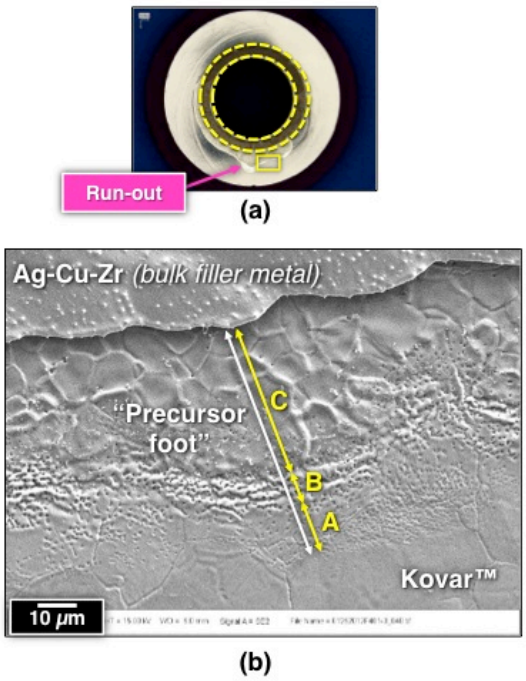

Figure 11 (a) Photograph shows a tensile button that was pull tested to reveal run-out on the Kovar™ spacer. The process conditions were 985°C, 5 min, and 600 torr Ar. (b) SEM (SE) image of the edge of the run-out taken in the yellow box of (a). A precursor foot developed that had three zones "A," "B," and "C" as distinguished by surface topography.

At the edge of the Ag-Cu-Zr filler metal is a "precursor foot" that is made visible by the high magnification, SEM image in Fig. 11b. The precursor foot, which extend approximately 40 µm from the bulk filler metal edge, has three zones labeled "A", "B", and "C" that are distinguished by the surface topography. Surface and near-surface (limited bulk) diffusion, together with the reaction, were the expressed mechanisms responsible for the precursor phenomenon.

The composition of the precursor foot was analyzed by the EDX analysis. The back scattered electron (BSE), SEM image, together with the Fe, Ni, and Al maps are shown in Fig. 12. The regions "B" and "C" exhibited a very strong presence of Al and an enrichment of Ni versus Fe when compared to unreacted Kovar™ at the lower, right-hand region of the image. Metallographic cross sections determined that the displaced Fe had concentrated in the reaction layer under the Ni-rich, aluminide layer observed at the surface. The "A" region has a reduced amount of Al that causes it to be, chemically, nearly indistinguishable from unreacted Kovar™ alloy. Zirconium was absent from the precursor foot with the exception of a one-or-two isolated particles. The extent of the precursor foot away from the bulk filler metal demonstrated the strong driving force for the diffusion/reaction process between Al, Ni, and, Fe.

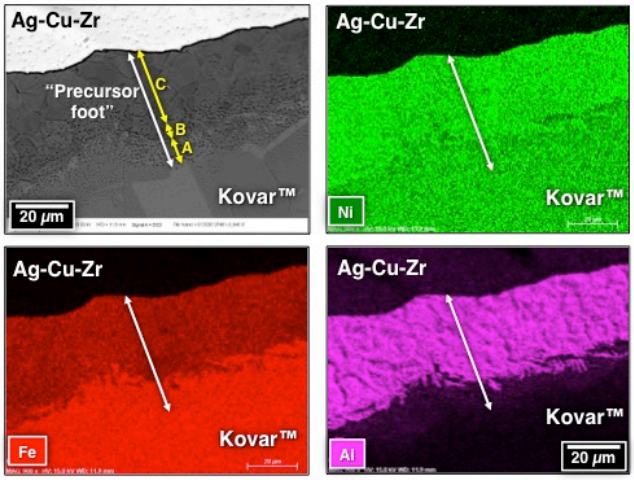

Figure 12 SEM (BSE) image and EDX analysis maps of Ni, Fe, and Al taken at the edge of the run-out analyzed in Fig. 11. The precursor foot and three surface topographies have been labeled in the SEM image.

A comparison was made between the precursor foot ahead of the run-out region as shown in Figs. 11 and 12, and the edge of the Ag-Cu-Zr fillet where run-out was absent. The latter structure was taken from the same sample as displayed in Fig. 11a, but at a different location that is shown by the yellow box in Fig. 13a. (The image in Fig. 13a image was rotated with respect to Fig 11a.) The SEM (SE) image is shown of the fillet edge in Fig.13b, which highlights the surface topography. The edge of the is comprised of an array of particles. The raised "plateau" in the upper right-hand corner is the fracture surface. The edge of the filler metal is very abrupt when compared to the gradual decrease of fillet thickness at the edge of the run-out in Fig. 11b.

The corresponding SEM (BSE) image is provided in Fig. 13c, which shows the compositional footprint of the fillet edge. There appear to be three distinct regions: two phases comprising the particle region and the filler metal matrix. The black contrast of the raised plateau is Al_2O_3 that was pulled out of the surface of the mating Al_2O_3 button by the pull test.

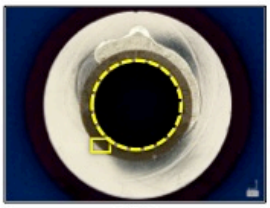

(a)

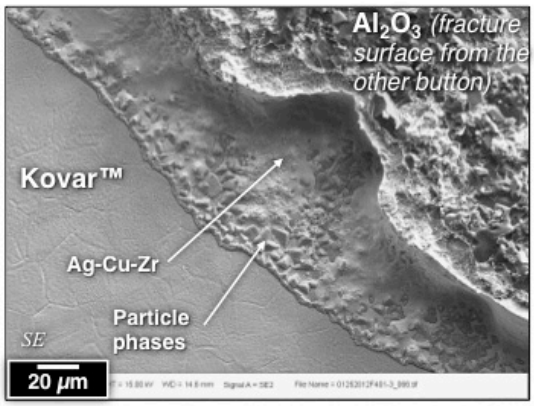

(b)

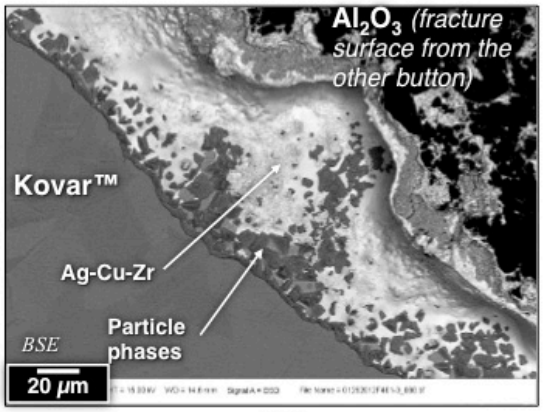

(c)

Figure 13 (a) Photograph shows a tensile button that was pull tested to reveal run-out on the Kovar™ spacer. The process conditions were 985°C, 5 min, and 600 torr Ar. (b) SEM (SE) image shows the edge of the wetted filler metal (yellow box) where run-out did *not* occur during brazing. (c) SEM (BSE) image was made of the same location as (b).

The EDX analysis was used to obtain a qualitative assessment of the phase phases present in Fig. 13. The x-ray maps are shown in Fig. 14 of the same, non-run-out region. The particle phases were comprised Fe and Ni as well as Zr and Al; the latter two elements appear to spatially compliment each-other. The particles of brighter gray tone were rich in Zr while the other particle phase was rich in Al; they represent the exposed zirconide and aluminide reactions, respectively. The matrix phase was the remaining Ag-Cu-Zr filler metal that was devoid of its Zr constituent.

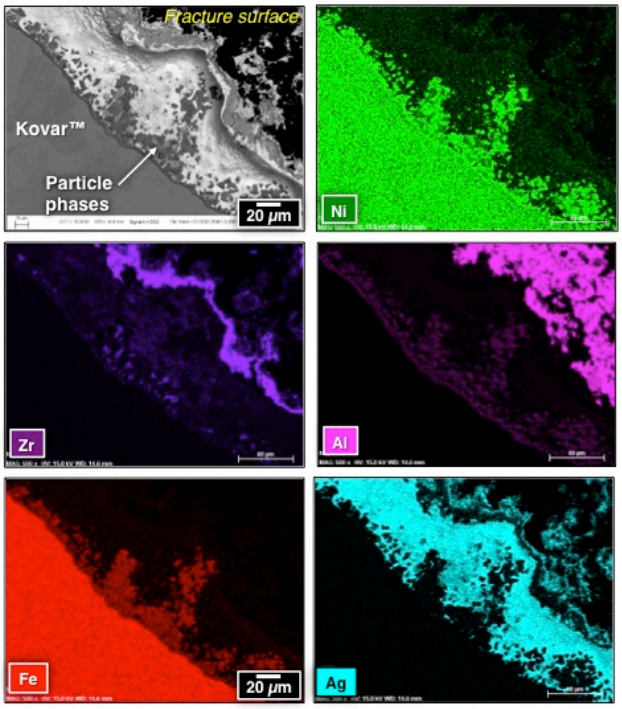

Figure 14 SEM/BSE image as well as Zr, Al, Fe, Ni, and Ag EDX maps are shown of the fillet edge where run-out was not observed on the Kovar™ spacer. The process conditions were 985°C, 5 min, and 600 torr Ar, pull test sample.

The EDX analysis in Fig. 14 allowed for labeling the likely compositions of the particle phases, which was performed in Fig. 15. Figure 15a repeats the same region of fillet edge without run-out. The high magnification image is provided in Fig. 15b that shows the particle phases and their proposed compositions. The dark particles predominate, which are the high-Al, $(Fe, Ni, Co)_x(Al, Zr)_y$ phase. This phase also appears to form a contiguous boundary along the perimeter of the fillet edge. The light-gray material is the high-Zr, $(Zr, Al)_y(Fe, Ni, Co)_x$ phase; it surrounds the high-Al particles. The filler metal was identified as Ag-Cu-Zr although the Zr component was lost to the interface and redox reactions.

The final analysis of the interface reactions examined the fillet edges by metallographic cross section. Shown in Fig. 16 are the SEM image as well as the Al and Zr EDX analysis maps that originated from a run-out region of the specimen shown in Figs. 11 and 12. The SEM image shows the raised edge that formed during solidification of the filler metal (black arrow). There was an extensive diffusion/reaction between Al and the Kovar™ constituents to a distance of about 50 μm ahead of the sessile drop edge (orange arrow), which corresponds to the surface morphology in Fig. 11b. It is presumed that the layer is the high-Al, $(Fe, Ni, Co)_x(Al, Zr)_y$ phase. It was not possible to discern specific microstructural features in Fig. 16 that were responsible for the individual zones "C," "B," and "A" belonging to the precursor foot in Fig. 11b other than they reflected gradually decreased thicknesses of the $(Fe, Ni, Co)_x(Al, Zr)_y$ layer.

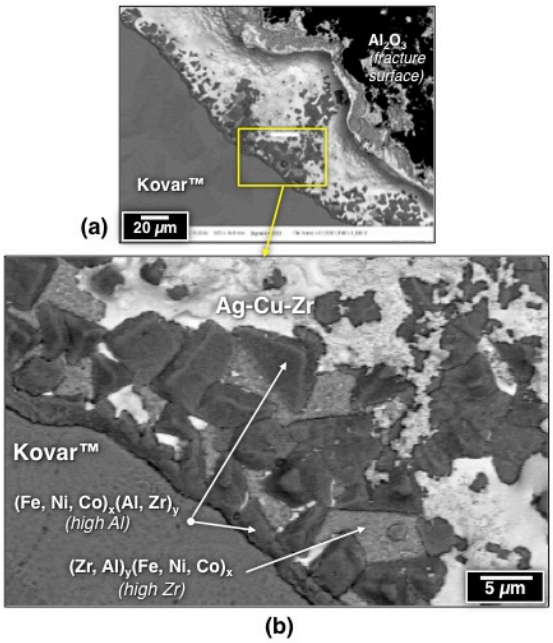

Figure 15 (a) Low magnification SEM (BSE) image shows the fillet edge of the pull test sample where run-out did not occur during brazing. The yellow box indicates the region of interest, which was the particle phases. (b) High magnification SEM (BSE) image shows the fillet edge. The particle phases have been identified with the most likely compositions.

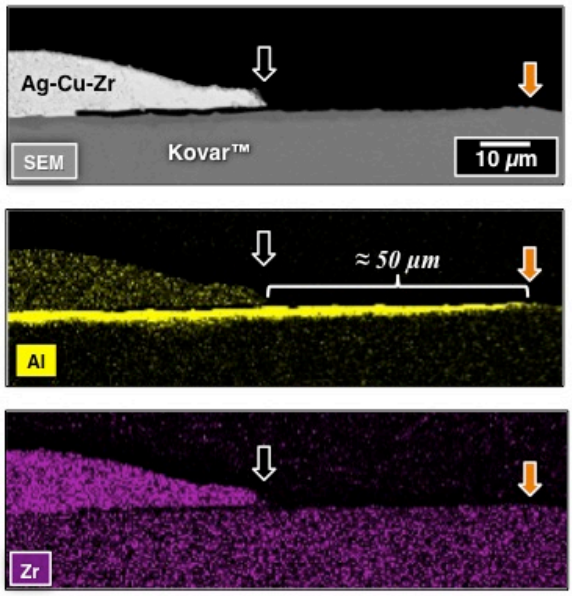

Figure 16 SEM image shows the edge of the Ag-Cu-Zr sessile drip at a *run-out location*. The process conditions were 985°C, 5 min, and 600 torr Ar. EDX maps of Al and Zr show the extent of the precursor foot (between the black and orange arrows) and that it was comprised of the high-Al, (Fe, Ni, $Co)_x(Al, Zr)_y$ phase that gradually decreased in thickness away from the filler metal edge.

A similar cross section was made of the Ag-Cu-Zr fillet edge at a location where run-out was absent. The corresponding images are shown in Fig. 17 that include an SEM photograph together with the Al and Zr EDX maps. The aluminide reaction layer extended approximately 16 μm from the fillet edge (black arrow) into the Kovar™ (orange arrow). The layer was comprised of the same large, high-Al, (Fe, Ni, $Co)_x(Al, Zr)_y$ phase particles ("A") that were observed in Fig. 15b. That phase also comprised the perimeter structure in Fig. 15b, that is now observed in-profile at location "B" of the Al map of Fig. 17. Unlike the run-out region, the high-Zr, $(Zr, Al)_y(Fe, Ni, Co)_x$ phase layer accompanied the high-Al phase to the same distance, being between the latter and the Kovar™ base material. Its surface morphology was shown in Fig. 15b.

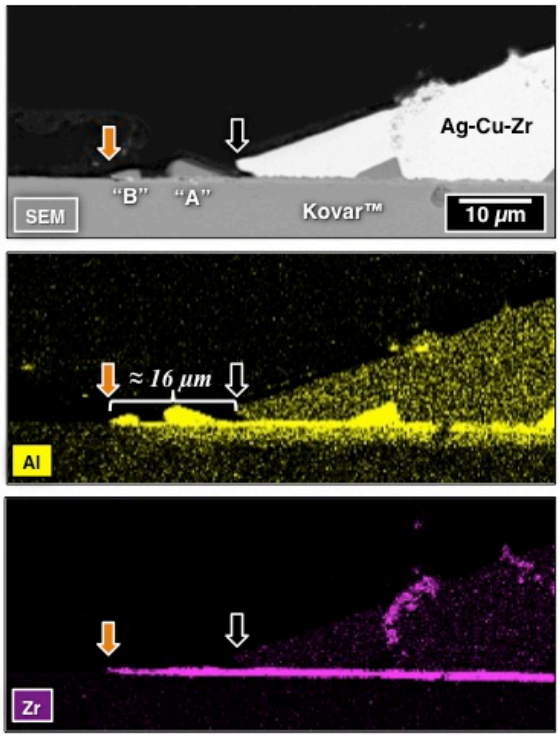

Figure 17 SEM image shows the edge of the Ag-Cu-Zr sessile drip at a *non-run-out location*. The process conditions were 985°C, 5 min, and 600 torr Ar. The EDX maps of Al and Zr show the extent of the diffusion/reaction by the high-Al and high-Zr phases (between the black and orange arrows).

A comparison was made between the images in Fig. 16 (run-out) and 17 (no run-out). The analysis indicates that co-formation of the high-Al, $(Fe, Ni, Co)_x(Zr, Al)_y$ *and* the high-Zr, $(Zr, Al)_y(Fe, Ni, Co)_x$ phase underneath it, impeded the diffusion/reaction of the high-Al phase from extending further from the filler metal edge as the precursor to run-out. The fact that the high-Zr layer was underneath the high-Al layer suggests that the former grew prior to the arrival of elemental Al from the redox reaction at the Ag-Cu-Zr/Al_2O_3 interface. This scenario implies that the source of the instability is formation of the high-Al, $(Fe, Ni, Co)_x(Al, Zr)_y$ phase when it is unchecked by the co-development of the high-Zr, high-Zr, $(Zr, Al)_y(Fe, Ni, Co)_x$ phase.

The above scenario indicates that run-out is stochastic in nature, similar to corrosion behavior. Run-out begins with a local perturbation in the system – e.g., in the case of the molten filler metal, either an excess of Al that drives the high-Al, $(Fe, Ni, Co)_x(Al, Zr)_y$ diffusion/reaction or a deficiency of Zr that fails to create the high-Zr, $(Zr, Al)_y(Fe, Ni, Co)_x$ phase.

At that point, the high-Al diffusion/reaction predominates, generating the precursor foot that locally accelerates wetting and spreading by the molten filler metal out, onto the Kovar™ base material surface. It cannot be ruled out that the system perturbation was caused by a local anomaly on the Kovar™ surface, although there was no explicit evidence to this effect. Clearly, there is a factor that limits run-out to one or two locations. One potential explanation is a drop in overall system free energy resulting from (a) the run-out diffusion/reaction, itself, and (b) a change to the surface energy of the molten filler metal. The latter contribution is a collaborative effect between the molten alloy surface tension and the joint geometry. The significance of the surface energy is investigated in the next section.

Base Material Geometry

The above analysis points to the aluminide reaction, when unchecked by the high-Zr reaction, as the underlying factor in the wetting and spreading instability responsible for run-out. The next analysis was performed to determine the extent to which, surface energy, which is controlled by the surface tension of the molten solder and joint geometry, has a role in the run-out phenomenon.

Test Specimens

Duplicate tensile button samples were fabricated that represented one of four variants constructed of different spacer and base materials. Those variants are represented schematically by the cells in Fig. 18. The upper left-hand cell represents the "All Kovar™" joint that has the individual buttons and the spacer fabricated from the alloy. To its right is the baseline variant – Al_2O_3 buttons and a Kovar™ spacer. The lower left-hand cell has Kovar™ buttons and an Al_2O_3 spacer, which is reverse to the traditional configuration. Lastly, there is the "All ceramic" sample that has all of the components constructed of Al_2O_3 ceramic base material.

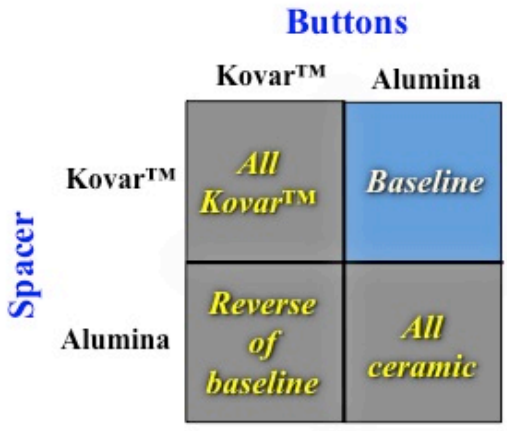

Figure 18 Schematic diagram shows the four variants of individual tensile button and spacer material when fabricated of Kovar™ or Al_2O_3.

A photograph of the test samples is shown in Fig. 19. The buttons and spacers were brazed together using a 0.002 in. thick preform of the Ag-Cu-Zr filler metal. The process conditions were 985°C, 5 min, and 600 torr Ar. The braze joint gap was controlled by dimples in the case of the Kovar™ spacer, and 0.001 in. ribbons when the Al_2O_3 spacer was in place.

Figure 19 Photograph shows the variants of the tensile button samples.

Each sample was inspected for the presence of run-out. Those results are summarized in Fig. 20. The baseline sample exhibited the expected run-out behavior. There was an absence of run-out in the all-Kovar™ braze joints. This finding confirms that the elemental Al released by the Zr/Al_2O_3 redox reaction is required for the run-out phenomenon to take place; it is not simply a physical displacement ("squishing out") of excess molten filler metal.

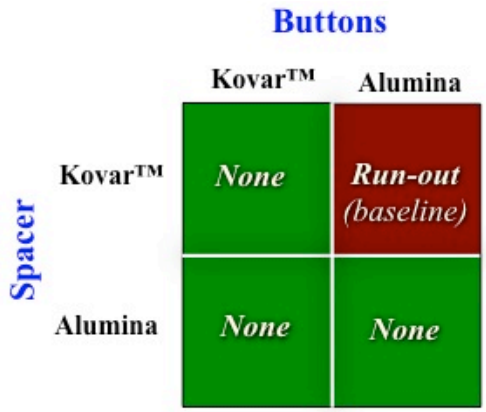

Figure 20 Schematic diagram shows the four variants between the spacer and button base materials.

The all-Kovar™ samples were examined by metallographic cross sections in order to determine the fate of the Zr component of the Ag-Cu-Zr filler metal. The microstructure of these braze joints is represented by the SEM image in Fig. 21. Reaction layers formed at both Ag-Cu-Zr/Kovar™ interfaces between Zr and the Fe, Ni, and Co constituents of the base material. Those reactions consumed all of the Zr content in the filler metal. The remaining filler metal contained Ag and the Cu constituent; the latter did not participate in the interface reaction.

There was a noticeable difference between the microstructures of the two reaction layers. That difference became less significant with decreasing gap thickness. There were no obvious reasons for the different layer morphologies. The EDX maps indicated that, qualitatively, the two layers had the same chemistry. The reaction layer compounds were heavier in Ni than in the Fe, despite the opposite proportionality of the two elements in the Kovar™ base material. The consequence was a slightly higher concentration of Fe in the Kovar™ immediately adjacent to the interface. Cobalt was also present in the reaction layers.

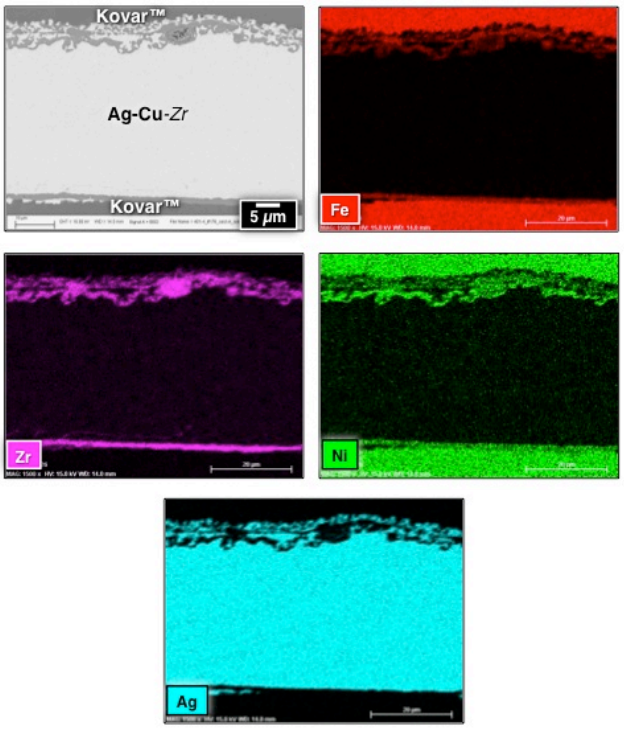

Figure 21 SEM image and EDX maps show the physical metallurgy and composition, respectively, of the Ag-Cu-Zr braze joint fabricated between the Kovar™ buttons and Kovar™ spacer.

This sample established, conclusively, that there is a significant driving force for Zr to react with the constituents of the Kovar™ base material. However, those reactions do not provide the driving force for the run-out phenomenon. The evidence to this effect is supported by the SEM image in Fig. 22. The cross section was taken of the fillet, just below the red dot in the inset photograph. The observable reaction layers extended as far as indicated by the yellow arrows. The filler metal wet and spread further onto, and up, the spacer and button, respectively, but not in a manner characteristic of run-out. Therefore, it is the aluminide reaction, not the zirconide reaction, that drives the run-out behavior when both can develop in the metal-ceramic braze joint.

The analysis turns to the samples having Kovar™ buttons, but a ceramic spacer. The SEM photographs in Fig 23 confirmed formation of the ZrO_2 zone that results from the redox reaction. It was expected that run-out would be observed, since the redox reaction generated elemental Al. But, such was not the case. Attention turned to the Ag-Cu-Zr/Kovar™ interface, which is shown in Figs 24a and 24b. This microstructure can be compared to Fig. 9. The high Al, $(Fe, Ni, Co)_x(Al, Zr)_y$ layer was absent that was located adjacent to the Kovar™ base material. The high-Zr, $(Zr, Al)_y(Fe, Ni, Co)_x$ alloy was observed along the entire interface and it was very thick. The second, high-Al layer occurred intermittently along the interface, being present as either isolated particles (Fig. 24b) or as a discontinuous layer. Although this Ag-Cu-Zr/Kovar™ interface structure was not typical as is shown Fig. 9, it was also not unusual amongst the many test specimens.

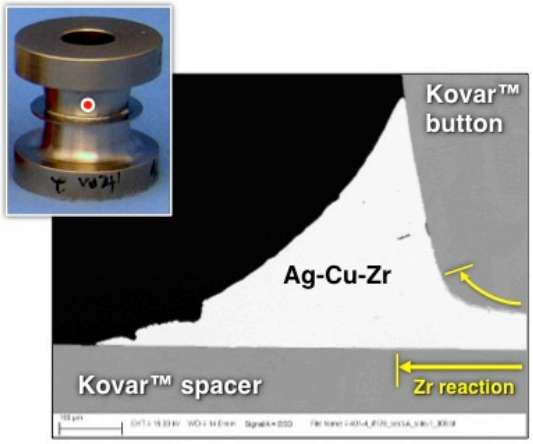

Figure 22 SEM image shows the cross section of the fillet that formed under the red dot of the inset photograph for the all-Kovar™ test sample made with the Ag-Cu-Zr filler metal. The yellow arrows indicate the extent of the zirconide reaction.

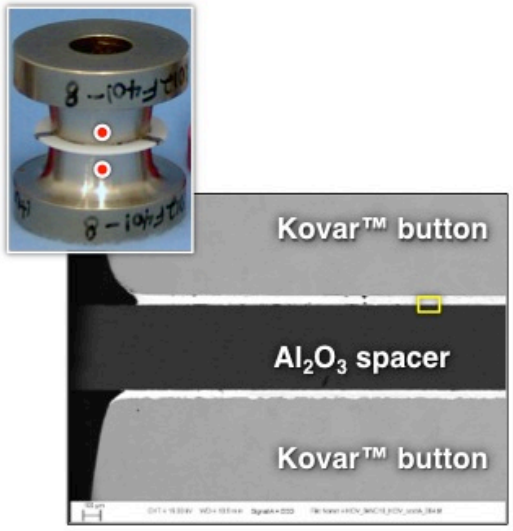

(a)

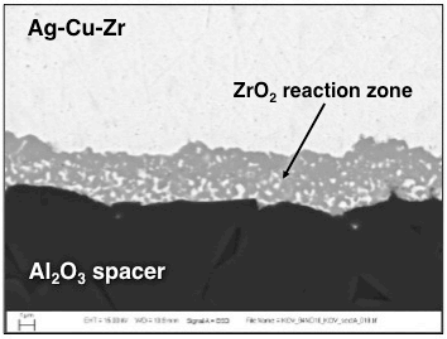

(b)

Figure 23 (a) SEM image shows the cross section of the Ag-Cu-Zr braze joint made between the Al_2O_3 spacer and the Kovar™ buttons. The inset photograph shows the sample; the cross section was made between the red dots. (b) High magnification SEM photograph shows the ZrO_2 reaction zone formed at the Ag-Cu-Zr/Al_2O_3 interface.

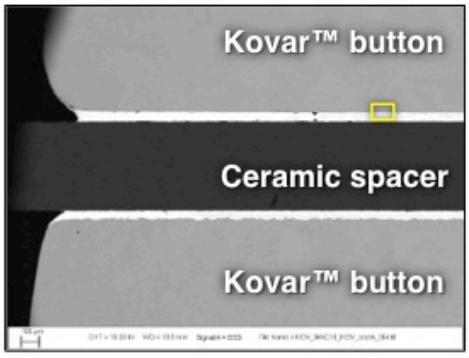

(a)

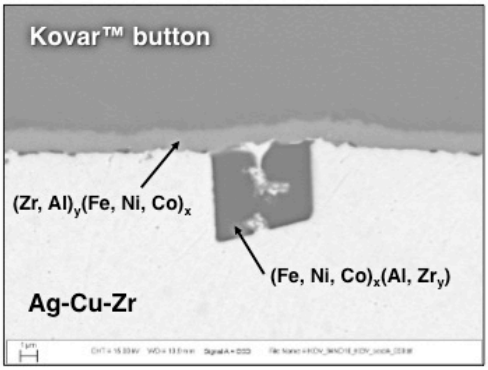

(b)

Figure 24 (a) SEM image shows the cross section of the Ag-Cu-Zr braze joint between the red dots of the inset photograph that illustrates the tensile button made with the Al_2O_3 spacer and Kovar™ buttons. (b) The SEM photograph shows the reaction layers that formed at the Ag-Cu-Zr/Kovar™ interface.

All of the physical metallurgy was in place to support a run-out event. The aluminide layer developed at the Ag-Cu-Zr/Kovar™ interface in the gap and extended through the fillets and well up the wall of the button in a manner indicative of the run-out phenomenon. This observation is illustrated in Fig. 25. The cross section of the Kovar™/Al_2O_3/ Kovar™ braze joint is repeated in Fig. 25a. The picture in Fig. 25b highlights the region in front of the fillet edge, which is shown in higher magnification in Fig. 25c. The corresponding EDX Al map, which is shown in Fig. 25d, confirmed that the aluminide diffusion/reaction had occurred well beyond the fillet edge.

The aluminide diffusion/reaction observed in Fig. 25 should have led to run-out up the wall of the button. The absence of the phenomenon was due to the geometry of the fillet region and the contributing factor of molten filler metal surface tension.[1] This point is described with the assistance of Fig. 26. The solid blue line marks the limit of the solder fillet. The fillet shape that would be required in the event of run-out up the button, is described by the dashed trace. The latter fillet configuration would require the filler metal to wet an additional distance "A" further out, on the Al_2O_3 surface. However, the Ag-Cu-Zr active braze alloy cannot spontaneously spread on the ceramic surface. Therefore, although the aluminide diffusion/reaction can progress up the sidewall of the Kovar™ button, uninhibited, the surface tension of the molten filler metal cannot permit the latter to follow the reaction layer to create a run-out lobe.

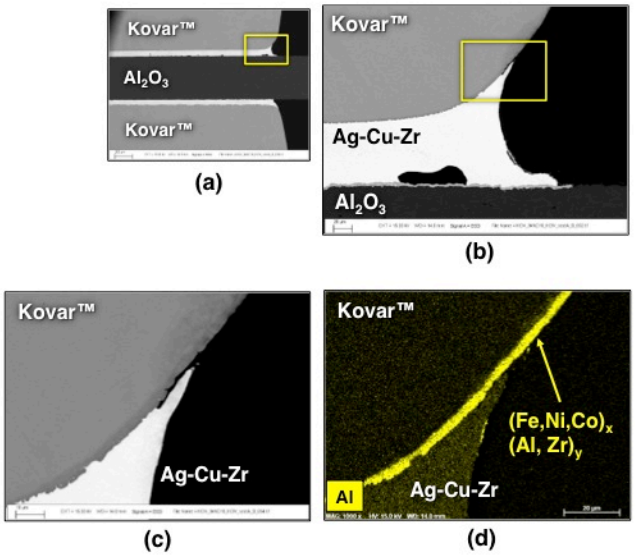

Figure 25 (a) SEM image shows the cross section of the Ag-Cu-Zr braze joint made between the Al_2O_3 spacer and the Kovar™ buttons. (b) The medium magnification image shows the top of the filler metal fillet. (c, d) SEM image and EDX map of Al illustrate the extent of the aluminide diffusion/reaction beyond the fillet edge.

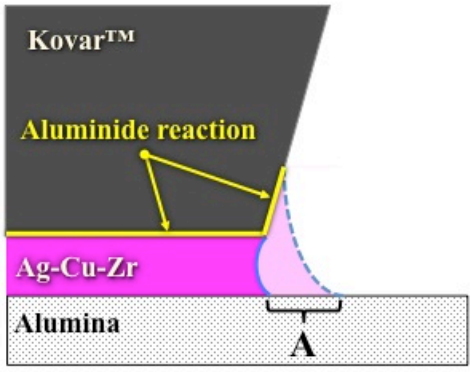

Figure 26 Schematic diagram shows the extension of the Ag-Cu-Zr braze alloy fillet, "A," that would be required for the molten filler metal to follow the aluminide diffusion/reaction up the sidewall of the Kovar™ button as run-out.

The final configuration in this experiment was the all-Al_2O_3 specimen. As expected, the redox reaction took place at both Ag-Cu-Zr/Al_2O_3 interfaces. Run-out was not observed on the Al_2O_3 surfaces, thereby confirming that the Kovar™ base material and, specifically, the aluminide reactions, were required for run-out to take place.

[1] Strictly speaking, interfacial tensions, of which the surface tension of the fillet is one part; joint geometry; and gravity control wetting and spreading by the molten filler metal.

In the absence of the Kovar™ base material, the Al_2O_3/Ag-Cu-Zr/Al_2O_3 provided the opportunity to measure the quantity of elemental Al generated by the redox reaction. Electron probe microanalysis (EPMA) was used to measure the concentrations of Al and Zr present in the filler metal field. One of the replicate traces is shown in Fig. 27.

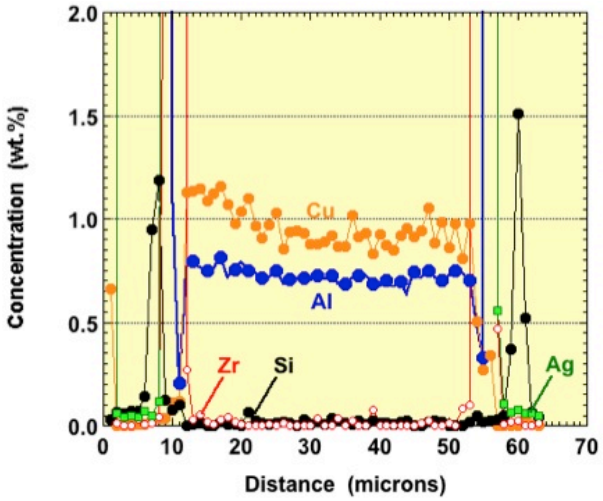

Figure 27 EPMA trace across the Al_2O_3/Ag-Cu-Zr/Al_2O_3 braze joint. The concentration scale was magnified in order to show the concentrations of Zr and Al in the bulk filler metal field.

The EPMA data confirmed that all of the 2 wt.% Zr component in the filler metal had been consumed by the redox reaction. In addition, the concentration of elemental Al resided was in the range of:

0.7 – 0.9 wt. % Al.

It is interesting that a relatively small quantity of elemental Al was responsible for the aluminide reactions and the run-out phenomenon observed in this brazement.

Lastly, this sample provide evidence with respect to the driving force behind the Zr/Al_2O_3 redox reaction. The absence of the Kovar™ base material eliminated the aluminide reactions as a contributor to that driving force. Therefore, it is concluded that either the free energy of solution, which results from elemental Al entering the filler metal, or an inaccuracy in the literature values of standard free energies of formation, was responsible for the spontaneity of the Zr/Al_2O_3 redox reaction.

In summary, the analysis of the mixed configuration, tensile buttons yielded important information regarding the run-out phenomenon: (a) The strong reaction between Zr and the constituent elements of the Kovar™ base material does not drive the run-out phenomenon. Rather, run-out is driven, expressly, by the aluminide reaction. (b) The geometry of the braze joint, in conjunction with the surface tension of the molten filler metal, can determine the presence or absence of run-out, even in the presence of the strong aluminide reaction layers.

Conclusions

1. The run-out behavior degraded braze joints made between Kovar™ and Al_20_3 ceramic using the active filler metal, 97Ag-2Zr-1Cu (wt. %). Because it did not respond to different parameters within the acceptable process window or to features added to the Kovar™ surface, a study was conducted to determine the root-cause of the underlying wetting and spreading instability as a first-step towards its mitigation.
2. Aluminum was released into the molten Ag-Cu-Zr filler metal by the redox reaction between Zr and the Al_2O_3 base material. The Al reacted with the Kovar™ constituents, creating an aluminide reaction layer that provided the primary driving force behind the wetting and spreading instability.
3. The surface tension of the molten Ag-Cu-Zr filler metal, in conjunction with the braze joint geometry, had a significant effect on the extent of the run-out.
4. The findings of this study indicate that the strategies having the greatest promise of successfully mitigating run-out are (a) alloy modifications to the filler metal, or (b) the use of coatings on the Kovar™ surface.

Acknowledgments

The authors wish to thank Lisa Deibler for her careful review of the manuscript. Sandia is a multiprogram laboratory operated by Sandia Corporation, a Lockheed Martin Company, for the United States Department of Energy's National Nuclear Security Administration under contract DE-AC04-94AL85000.

References

[1] ASTM F19-11, "Standard Test Method for Tension and Vacuum Testing Metallized Ceramic Seals," (West Conshohocken, PA; 2011).

[2] "The Ag-Al (Silver-Aluminum) System," ed. by A. McAlister, *Bull. of Alloy Phase Diagrams,* Vol. 8, No. 6 (1987), p. 526.

[3] Yue, T., Yang, H., Li, T., and Huang, K., "The Synthesis of Graded Thermal Barrier Coatings on Nickel Substrates by Laser Induced Thermite Reactions," *Mater. Trans. Jap. Inst. of Metals*, Vol. 50, No. 1 (2009), pp. 219-221.